Nonlinear pulse compression stage delivering 43-W few-cycle pulses with GW peak-power at 2-μm wavelength

Martin Gebhardt, Christian Gaida, T. Heuermann, F. Stutzki, C. Jauregui, et al.

Martin Gebhardt, Christian Gaida, T. Heuermann, F. Stutzki, C. Jauregui, J. Antonio-Lopez, A. Schülzgen, R. Amezcua-Correa, A. Tuennermann, J. Limpert, "Nonlinear pulse compression stage delivering 43-W few-cycle pulses with GW peak-power at 2-μm wavelength," Proc. SPIE 10512, Fiber Lasers XV: Technology and Systems, 105120V (26 February 2018); doi: 10.1117/12.2288685

SPIE.

Event: SPIE LASE, 2018, San Francisco, California, United States

Nonlinear pulse compression stage delivering 43-W few-cycle pulses with GW peak-power at 2-µm wavelength

Martin Gebhardt,[1,2*] Christian Gaida,[1] T. Heuermann,[1,2] F. Stutzki,[1] C. Jauregui,[1]
J. Antonio-Lopez,[3] A. Schulzgen,[3] R. Amezcua-Correa,[3]
A. Tünnermann[1,2,4] and J. Limpert,[1,2,4]

1 Institute of Applied Physics, Abbe Center of Photonics, Friedrich-Schiller-Universität Jena, Albert-Einstein-Str. 15, 07745 Jena, Germany
2 Helmholtz-Institute Jena, Fröbelstieg 3, 07743 Jena, Germany
3 CREOL, College of Optics and Photonics, University of Central Florida, Orlando, Florida 32816, USA
4 Fraunhofer Institute for Applied Optics and Precision Engineering, Jena, Germany
+now with Fraunhofer Institute for Applied Optics and Precision Engineering

*martin.gebhardt@uni-jena.de

ABSTRACT

In this contribution we demonstrate the nonlinear pulse compression of an ultrafast thulium-doped fiber laser down to 14 fs FWHM duration (sub-3 optical cycles) at a record average power of 43 W and 34.5 µJ pulse energy. To the best of our knowledge, we present the highest average power few-cycle laser source at 2 µm wavelength. This performance level in combination with GW-class peak power makes our laser source extremely interesting for driving high-harmonic generation or for generating mid-infrared frequency combs via intra-pulse frequency down-conversion at an unprecedented average power.
The experiments were enabled by an ultrafast thulium-doped fiber laser delivering 110 fs pulses at high repetition rates, and an argon gas-filled antiresonant hollow-core fiber (ARHCF) with excellent transmission and weak anomalous dispersion, leading to the self-compression of the pulses. We have shown that ARHCFs are well-suited for nonlinear pulse compression around 2 µm wavelength and that this concept features excellent power handling capabilities. Based on this result, we discuss the next steps for energy and average power scaling including upscaling the fiber dimensions in order to fully exploit the capabilities of our laser system, which can deliver several GW of peak power. This way, a 100 W-class laser source with mJ-level few-cycle pulses at 2 µm wavelength is feasible in the near future.

Keywords: Nonlinear pulse compression, nonlinear broadening, fiber laser, mid-IR laser

1. INTRODUCTION

Ultrafast lasers emitting at around 2 µm wavelength have become important tools for lots of applications in spectroscopy [1], metrology [2] and material processing [3]. Recently, there has been a large effort aimed at scaling the performance of these laser systems to transform them into mature drivers for high-field experiments and nonlinear frequency conversion processes, which require high peak intensities.

Such laser systems enable the generation of high harmonics (HHG) with high photon energies [4] because of the fact that the ponderomotive potential of the laser field is proportional to the square of its wavelength. One important requirement for a laser to efficiently drive high cut-off HHG is to deliver few-cycle pulses, because that allows focusing down to high peak intensities (leading to a high conversion efficiency and a high photon energy cut-off [5]) without losing the phase-matching by undesired ionization. Additionally, a few-cycle driver facilitates the generation of isolated attosecond pulses [6]. Resulting from the recent progress in laser development, HHG sources driven by few-cycle 2 µm

Fiber Lasers XV: Technology and Systems, edited by Ingmar Hartl, Adrian L. Carter, Proc. of SPIE
Vol. 10512, 105120V · © 2018 SPIE · CCC code: 0277-786X/18/$18 · doi: 10.1117/12.2288685

laser systems have led to cutting-edge results such as the time-resolved observation of light-induced chemical reaction paths [7] and X-ray absorption edge spectroscopy of organic molecules [4].

Similarly, high-power 2 μm laser systems with few-cycle pulse durations are of paramount interest for generating ultra-broad mid-infrared (mid-IR) phase-stable frequency combs due to intra-pulse difference frequency generation (DFG) [8, 9]. It is important to start with very short pulses coming from the driving laser to provide chirp-free frequency components with wide spectral separation such that the generated mid-IR DFG spectra can extend to short wavelengths. With respect to the mid-IR bandwidth and power, it is very beneficial to drive the frequency conversion at around 2 μm wavelength, as this allows using non-oxide nonlinear crystals that offer high nonlinearity, broad phase-matching and, most importantly, excellent spectral transmission up to 20 μm wavelength. A laser source addressing such broad mid-IR spectral ranges with powerful, phase-stable ultrashort pulses is extremely interesting for high-sensitivity and high-precision fingerprint absorption spectroscopy.

Certainly, the always-growing number of applications that greatly benefit from intense few-cycle laser sources operating beyond the well-explored near-infrared wavelength region leads to a strongly increased demand for these sources to deliver more average power. In particular, the above-mentioned applications can be significantly improved (e.g. in terms of signal-to-noise ratio and data acquisition times) if higher HHG photon-flux or mid-IR power can be reached.

The traditional approach for the generation of energetic few-cycle laser pulses at around 2 μm wavelength relies on nonlinear parametric amplification [10, 11]. However, scaling this concept to significantly more than ten watts has so far remained challenging because of the complexity of the pump sources, as well as due to the transmission and the properties of the oxide-based crystals. As opposed to that, we have recently introduced an alternative approach that is based on nonlinear compression of ultrashort pulses generated by high-repetition rate thulium-doped fiber laser systems [12, 13]. To date, these laser systems are capable of delivering ultrashort pulses with more than 100 W of average power [14] and GW-class pulse peak power with about 200 fs pulse duration [15]. In fact, nonlinear pulse compression (NPC) in the two micron wavelength region has also been investigated starting from solid-state and nonlinear parametric amplifiers [16, 17]. However, as mentioned above, the available average power was limited to a few watts by the driving laser.

In this contribution, we report on nonlinear self-compression of ultrashort pulses from a thulium-doped fiber laser using a gas-filled antiresonant hollow-core fiber (ARHCF). The key features to the pulse evolution in the experiment presented herein are the broad gain bandwidth of the active medium [18], allowing for clean 110 fs pulses from the laser system itself as well as the excellent transmission and weak anomalous dispersion of the ARHCF, leading to self-compression of the spectrally broadened pulses. We have generated 34.4 μJ-pulses with a FWHM duration of only 13 fs and a pulse peak power of 1.4 GW at a central wavelength of 1.82 μm. The combination of two average power scalable concepts for the generation and the post-compression of ultrashort pulses in this wavelength region is the key to high-power operation, allowing for an average power of 43 W. This is, to the best of our knowledge, the highest average power reported for any two micron few-cycle laser source to date.

2. EXPERIMENTAL SETUP

A schematic of the experimental setup can be seen in Fig. 1. The laser source, which enabled the experiments presented herein, was a thulium-doped fiber chirped-pulse amplification system (Tm:FCPA) with an architecture similar to the one described in Ref. [15]. As compared to this earlier reported work, we have increased its spectral bandwidth to about 140 nm, which was possible thanks to an improved stretcher and compressor design as well as the broad gain-bandwidth of thulium-doped silica. The spectrum was centered around 1920 nm wavelength, which ultimately means that detrimental propagation effects arising from the absorption lines of atmospheric water vapor have to be circumvented [19]. Regarding the thermal lens arising from water vapor absorption in a gaseous atmosphere, also described as thermal blooming, it was found that the best mitigation is to reduce the pressure of the medium in which the beam propagates [13]. Hence, the high-power sections of the laser system were enclosed in a vacuum chamber that was held at a pressure below 0.1 mbar. When adapted for the nonlinear compression experiments, the Tm:FCPA delivered 51 W of average power, corresponding to 41 μJ of pulse energy at a repetition rate of 1.25 MHz. Its output pulse duration (FWHM) was 110 fs. The measured pulse spectrum as well as an intensity autocorrelation trace are depicted in Fig. 2 and Fig. 3, respectively (orange line).

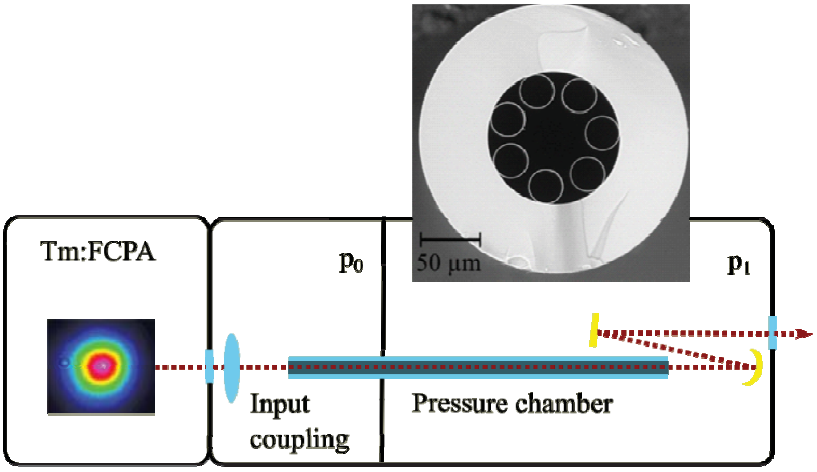

Figure 1. Experimental setup for the nonlinear pulse compression experiments comprising the laser output and two separate chambers filled with gas at pressures p_0 and p_1 (connected by the ARHCF)

The NPC stage consisted of two gas-filled pressure chambers that were connected by the ARHCF. The first one, which we here denote as the input coupling chamber, was filled with neon gas at a pressure of $p_0 = 0.4$ bar. This is a trade-off between two opposing requirements. On the one hand, low particle densities, providing a small thermo-optical coefficient, are desirable for the mitigation of thermal blooming, which otherwise reduces the coupling efficiency to the hollow fiber fundamental mode [13]. On the other hand, though, it is important to perform the input coupling in a medium that provides enough thermal conductivity such that the small but inevitable coupling-losses and the associated heat load close to the fiber tip have no effect on the stability and robustness of the fiber mode excitation at high average power. A higher gas pressure means a higher thermal conductivity [20]. We successfully found a balanced operation regime that fulfills both opposing requirements by choosing a light noble gas with a rather low pressure. The fiber itself was a node-less 7-capillary, antiresonant hollow-core fiber [21, 22]. It was fabricated in-house at CREOL, the University of Central Florida using OH-reduced silica glass. A cross-section of the fiber is depicted in Fig. 1. It had an inner core diameter of 53 µm and a core wall thickness of 535 nm. For the experiments presented herein, we used a length of 42 cm. The fiber design provides low-loss broadband transmission, especially at wavelengths spanning from 1.5 µm to 3.0 µm. Consequently, we have achieved >90% transmission through the ARHCF, including coupling losses. The output of the ARHCF was located within a second pressure chamber that was filled with argon gas at a pressure $p_1 = 3$ bar, which is close to the maximum pressure handling capabilities of the mechanical components in use. In order to circumvent chromatic aberrations and undesired dispersive effects, we used a spherical gold mirror to collimate the light emerging from the fiber output. Before characterization, the shortened pulses went through a 1 mm thick OH-reduced fused silica piece of glass, which served as an output window of the pressure chamber.

3. EXPERIMENTAL RESULTS

Similar to earlier experiments [16, 23] the pulse evolution along the ARHCF was dominated by the interplay of self-phase modulation induced spectral broadening and simultaneous temporal compression due to the anomalous waveguide dispersion. Thus, strong spectral broadening with a 20 dB width of about 800 nm was observed after the NPC stage, as can be seen in Fig. 2 (black line). The output pulse spectrum features a sharp edge at around 1300 nm, which corresponds to the short wavelength boundary of the ARHCF transmission window. Furthermore, Fig. 2 shows that the spectral center of mass was blue-shifted (to about 1820 nm). We found that the reason for this observation was the onset of ionization within the last few cm of the ARHCF, where the pulses are almost fully compressed, leading to a noticeable spectral blue-shift [24]. This behavior and the fact that the spectral guidance of the ARHCF was clamped to >1300 nm caused a slight decrease in the overall transmission to about 84% in high-power operation. The NPC output average

power was 43 W, corresponding to 34.4 µJ of pulse energy. An image of the collimated output beam profile showing no signature of thermal blooming at this performance level is depicted in Fig. 2.

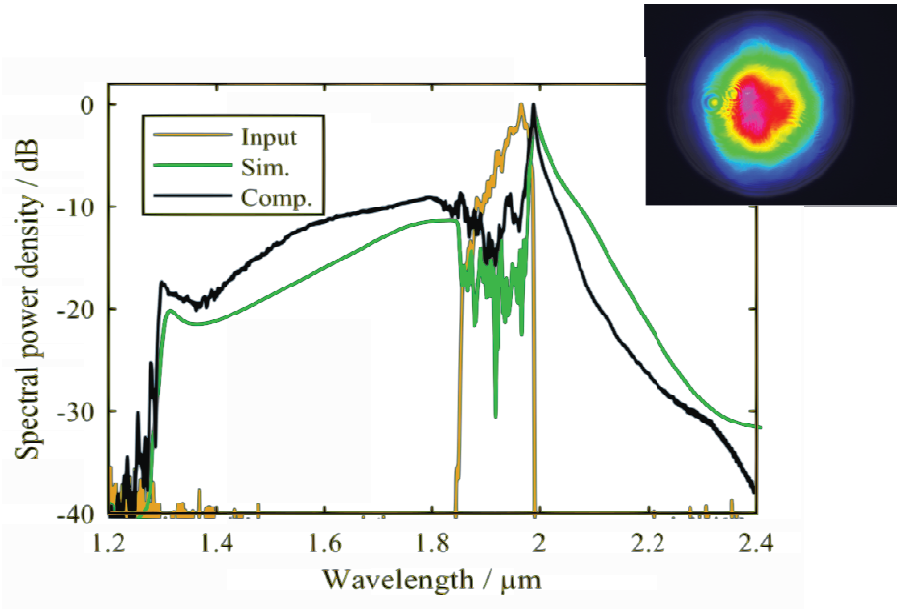

Figure 2. Measured pulse spectra at the NLC stage input (orange) and its compressed output (Comp., black) together with simulation results (Sim., green). Inset: image of the collimated output beam profile

The temporal characterization of the NPC output was performed using two different autocorrelation (AC) techniques. As can be seen in Fig. 3, we have achieved a significant temporal pulse compression of the NPC input (orange line) as compared to the compressed output (black line). The FWHM duration of the intensity AC trace measured after the NPC stage was <20 fs, which indicates a few-cycle pulse duration. In order to confirm this result, we have also performed an interferometric AC measurement using a different autocorrelator. The result of this measurement can be seen in the inset of Fig. 3. The black curve shows exactly five maxima and thus, four fringe periods within the FWHM time span of the main temporal feature. The duration of one fringe period corresponds to the duration of the electric field cycle, which is in our case 6.1 fs (as can be calculated from the central wavelength of 1820 nm). Like in the case of the intensity AC measurement, an appropriate deconvolution factor has to be found before the FWHM pulse duration or the number of electric field cycles within this time span can be accurately determined.

In order to gain a deeper understanding of the underlying physical processes and to derive the output pulse duration as well as the pulse peak power, we have performed a numerical simulation of the pulse evolution along the NLC stage. In the following, the important features of our simulation tool based on the split-step Fourier method will be summarized. This model describes the pulse evolution in the slowly evolving wave approximation [25] and it includes ionization effects that can cause a sudden change of the temporal nonlinear refractive index across the pulse introduced by the behavior of free carriers as described by the Drude model [24, 26]. The ionization rates are calculated using the Ammosov–Delone–Krainov model [27]. To describe the fiber dispersion across the very broad spectrum, we use the wavelength dependent refractive index distribution (rather than a Taylor expansion to a few orders) that is approximated based on the capillary model [28]. Additionally, we approximate the ARHCF resonance present at <1300 nm with a super Gaussian absorption band and we calculate the associated refractive index change according to the Kramers-Kronig relations. Of course, complete knowledge of the spectral refractive index distribution for the fundamental fiber mode requires finite-element simulations, but we believe that the model used in this work describes the experiments very well, especially because of the large core diameter. It reproduces our experimental observations, as can be seen when comparing the measurements (black line) and the simulation results (green line) in the spectral and temporal domains in Fig. 2 and Fig. 3, respectively.

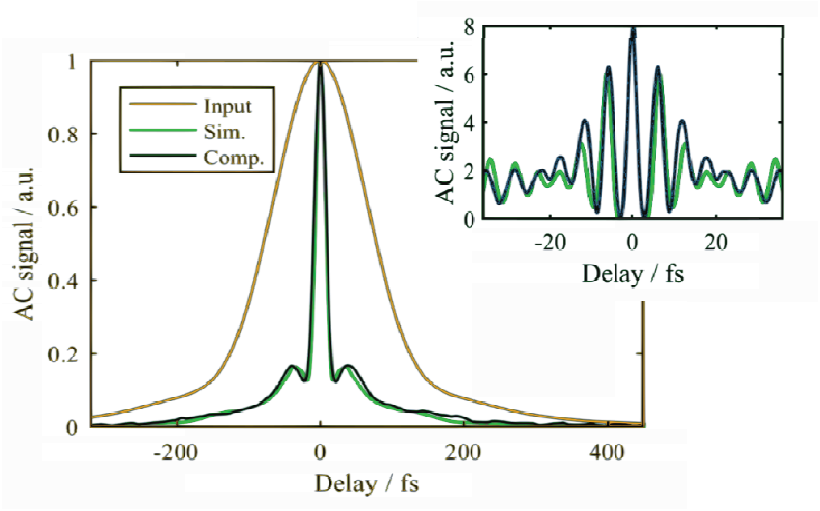

Figure 3 Measured intensity AC traces at the input (orange) and compressed output (Comp., black) of the NLC stage together with simulation results (Sim., green). Inset: interferometric AC measurement (black) and simulation results (green)

The FWHM duration of the numerical intensity AC is 16.3 fs, which is slightly shorter than the measurement. However, because of the good agreement between the simulation and the experiment it is a good estimation to use the numerically found autocorrelation deconvolution factors and energy content within the main temporal feature to retrieve the pulse duration and peak power obtained in the experiment. Hence, the accurate evaluation of our experimental measurements is not based on an assumption of the pulse profile but on the understanding of the pulse evolution along the ARHCF and its numerical simulation, which provide essential information. With this approach, we have retrieved a FWHM pulse duration of 19.6 fs/1.51 = 13.0 fs from the intensity AC, which corresponds to 2.1 optical cycles. The interferometric AC measurement showed four fringe periods within the FWHM duration, which yields 4/1.84 = 2.2 optical cycles. We believe that the difference in the temporal measurements arises from the slightly different propagation distances through air within our characterization setup. In the simulation result, about 60% of the pulse energy is confined within the main temporal feature of the pulse. Hence, we calculated that a pulse peak power was about 1.4 GW in the experiment described herein. Such peak power levels imply that the peak intensity at the end of the fiber was getting close to the magnitude of 10^{14} W/cm², which agrees well with the fact that we have already observed ionization. These ionization effects prevent further spectral broadening and temporal pulse shortening by increasing the nonlinear phase accumulation in our case, because they lead to a break-up of the pulse [29]. We have observed such pulse break-up in the experiment as well as in the simulation when the pulse energy or the fiber length were further increased, respectively.

Fig. 4 depicts the simulated pulse profile (green line) to give the reader an impression of the temporal power envelope of the pulses, which are available for experiments (i.e. after the pulses have left the pressure chamber at the NPC-stage output). The few-cycle pulse is riding on top of a weak pedestal, which is inherent to temporal self-compression. In fact, the modulation of this pedestal extending from a delay of 20 fs up to 60 fs after the intense main feature arises from the aforementioned edge of the fiber transmission window and its impact on the spectral phase as governed by the Kramers-Kronig relations. The input pulse envelope for the simulation is represented by the orange line and shows the strong peak power enhancement after the NPC stage. We have also retrieved the temporal phase from our simulation results, which can be seen in Fig. 4. It is well-behaved and almost linearly decreasing across the intense main feature. That correlates well to the fact that we found that the pulse duration of our simulated pulse is almost identical to the duration of the transform-limited pulse that can be expected from the measured spectrum.

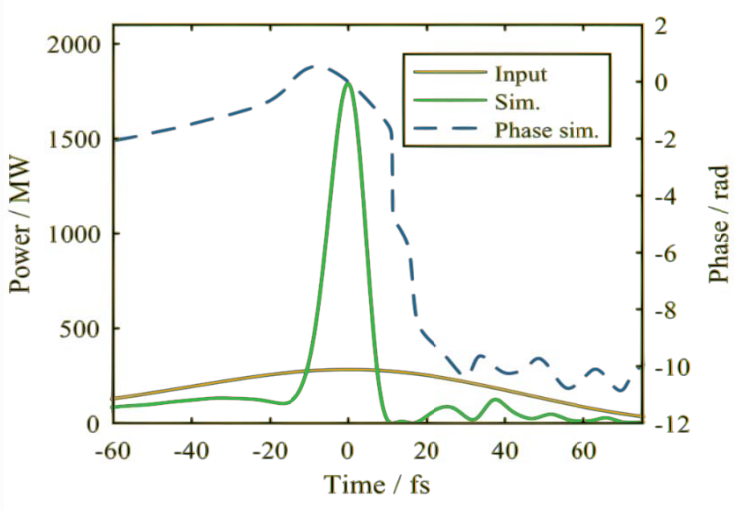

Figure 4. Simulation result of the temporal pulse profile after the NLC stage (Sim., green), together with the simulated temporal phase (Phase sim., green dashed) and a comparison with the input pulse (orange)

4. CONCLUSION AND OUTLOOK

To the best of our knowledge, we have presented the highest average power few-cycle laser source at 2 µm wavelength. This performance level in combination with GW-class peak power makes this source extremely interesting for driving HHG or for generating mid-IR frequency combs via intra-pulse frequency down-conversion at an unprecedented average power.

The work presented herein was enabled by a high-repetition rate ultrafast thulium-doped fiber laser system, i.e. an average power scalable laser concept. The laser system used in this experiment delivered 110 fs pulses. In fact, it can be expected that these pulse durations will further decrease as the spectral bandwidth of our laser system was only limited by the transmission of the optical elements. We have shown that ARHCFs are well-suited for nonlinear pulse compression around 2 µm wavelength and that this concept features excellent power handling capabilities. In order to fully exploit the potential of ultrafast Tm:FCPAs, our future work will include using larger hollow-core fibers with optimized spectral transmission. This way, a 100 W-class laser source with mJ-level few-cycle pulses at 2 µm wavelength is feasible in the near future.

The research leading to these results has been partly supported by the German Federal Ministry of Education and Research (BMBF) under contract “NUKLEUS” (13N13973), the United States AFOSR (FA9550-15-10041) and United States ARO (W911NF-12-1-0450). F.S. acknowledges support by the Carl-Zeiss Stiftung. M. G. achnowledges support by the Helmholtz-Institute Jena.

REFERENCES

1. A. Stark, L. Correia, M. Teichmann, S. Salewski, C. Larsen, V.M. Baev, P.E. Toschek, Opt. Comm., 215(1), 113-123 (2003).
2. K. Scholle, E. Heumann and G. Huber, Laser Phys. Lett. 1(6) 285 (2004).
3. I. Mingareev, N. Gehlich, T. Bonhof, A. Abdulfattah, A.M. Sincore, P. Kadwani, L. Shah, M. Richardson, Int. J. Adv. Manuf. Technol. 84(9-12) 2567-2578 (2015)
4. S. L. Cousin, F. Silva, S. Teichmann, M. Hemmer, B. Buades, and J. Biegert, Opt. Lett. 39, 5383 (2014).
5. S. Kazamias, S. Daboussi, O. Guilbaud, K. Cassou, D. Ros, B. Cros, and G. Maynard, Phys. Review A, 83, 063405 (2011).
6. F. Silva, S. M. Teichmann, S. L. Cousin, M. Hemmer, and J. Biegert, Nat. Comm. 6, 6611 (2015).
7. Y. Pertot, C. Schmidt, M. Matthews, A. Chauvet, M. Huppert, V. Svoboda, a. von Conta, A. Tehlar, D. Baykusheva, J.-P. Wolf, H. J. Wörner, Science, 355(6322), 264-267 (2017).
8. I. Pupeza, D. Sánchez, J. Zhang, N. Lilienfein, M. Seidel, N. Karpowicz, T. Paasch-Colberg, I. Znakovskaya, M. Pescher, W. Schweinberger, V. Pervak, E. Fill, O. Pronin, Z. Wei, F. Krausz, A. Apolonski, and J. Biegert, Nature Photonics, 9(11), 721–724 (2015).
9. J. Zhang, K. Mak, N. Nagl, M. Seidel, D. Bauer, D. Sutter, V. Pervak, F. Krausz, and O. Pronin, , submitted to Nature Photonics (2017).
10. Y. Shamir, J. Rothhardt, S. Hädrich, S. Demmler, M. Tschernajew, J. Limpert, and A. Tünnermann, Opt. Lett. 40, 5546-5549 (2015).
11. K.-H. Hong, S.-W. Huang, J. Moses, X. Fu, C.-J. Lai, G.Cirmi, A. Sell, E. Granados, P. Keathley, and F. X. Kärtner, Opt. Express 19, 15538-15548 (2011).
12. M. Gebhardt, C. Gaida, S. Hädrich, F. Stutzki, C. Jauregui, J. Limpert, and A. Tünnermann, Opt. Lett. 40, 2770-2773 (2015).
13. M. Gebhardt, C. Gaida, F. Stutzki, S. Hädrich, C. Jauregui, J. Limpert, and A. Tünnermann, Opt. Lett. 42, 747-750 (2017).
14. F. Stutzki, C. Gaida, M. Gebhardt, F. Jansen, A. Wienke, U. Zeitner, F. Fuchs, C. Jauregui, D. Wandt, D. Kracht, J. Limpert, and A. Tünnermann, Opt. Lett. 39, 4671-4674 (2014).
15. C. Gaida, M. Gebhardt, F. Stutzki, C. Jauregui, J. Limpert, and A. Tünnermann, Opt. Lett. 41, 4130-4133 (2016).
16. T. Balciunas, C. Fourcade-Dutin, G. Fan, T. Witting, A. A. Voronin, A. M. Zheltikov, F. Gerome, G. G. Paulus, A. Baltuska, and F. Benabid, Nat. Comm. 6, 6117 (2015).
17. K. Murari, G. J. Stein, H. Cankaya, B. Debord, F. Gérôme, G. Cirmi, O. D. Mücke, P. Li, A. Ruehl, I. Hartl, K.-H. Hong, F. Benabid, and F. X. Kärtner, Optica 3, 816-822 (2016).
18. S.D. Jackson, T. King, J. Lightwave Technol. 17, 948- (1999)
19. M. Gebhardt, C. Gaida, F. Stutzki, S. Hädrich, C. Jauregui, J. Limpert, and A. Tünnermann, Opt. Express 23, 13776-13787 (2015).
20. V. Antonetti, A. Bar Cohen, A. Bergles, L. Fletcher, J. Howell, J. Johnston, D.A. Kaminski, A. Kraus, F. Kreith, R. Lahey, S. Pantankar, M. Shah, and J. Weisman, Section 410.2 in *Fluid Flow Databook*, (General Electric, Genium Publishing, 1982), pp. 1 – 60.
21. W. Belardi and J. C. Knight, Opt. Express 22, 10091-10096 (2014).
22. F. Yu and J. C. Knight, Opt. Express 21, 21466-21471 (2013).
23. C. Gaida, M. Gebhardt, F. Stutzki, C. Jauregui, J. Limpert, and A. Tünnermann, Opt. Lett. 40, 5160-5163 (2015).
24. M. F. Saleh, W. Chang, P. Hölzer, A. Nazarkin, J. C. Travers, N. Y. Joly, P. St. J. Russell, and F. Biancalana, Phys. Rev. Lett. 107, 203902 (2011).
25. T. Brabec and F. Krausz, Phys. Rev. Lett. 78, 3282 (1979).
26. W. Chang, A. Nazarkin, J. C. Travers, J. Nold, P. Hölzer, N. Y. Joly, and P. St.J. Russell, Opt. Express 19, 21018-21027 (2011).
27. M.V. Ammosov, N.B. Delone, and V.P. Krainov, Sov. Phys. JETP 64(6), 1191-1194 (1986).
28. J. C. Travers, W. Chang, J. Nold, N. Y. Joly, and P. St. J. Russell, J. Opt. Soc. Am. B 28, A11-A26 (2011).C. I. Blaga, F. Catoire, P. Colosimo, G. G. Paulus, H. G. Muller, P. Agostini, and L. F. DiMauro, Nat. Phys. 5, 335 (2009).
29. P. Hölzer, W. Chang, J.C. Travers, A. Nazarkin, J. Nold, N.Y. Joly, M.F. Saleh, F. Biancalana, P.S.J. Russell, Phys. Review Lett. 107(20), 203901 (2011).